RADAB

Radiation action on bio-molecules

Invited lectures

Dynamics of Elementary Processes in the Gas Phase O_2 and CO

M.C. Bacchus-Montabonel[1], Y.S. Tergiman[1], N. Vaeck[2], E. Baloitcha[3] and M. Desouter-Lecomte[3,4]

1: Laboratoire de Spectrométrie Ionique et Moléculaire (UMR 5579 du CNRS) Université Lyon I, 43 Bd du 11 Novembre 1918, 69622 Villeurbane Cedex, France
2: Laboratoire de Chimie Physique Moléculaire, Université Libre de Bruxelles, CP 160/09, B-1050 Bruxelles
3: Laboratoire de Dynamique Moléculaire, Université de Liège, Institut de Chimie B6, Sart-Tilman, Liège 1, Belgique
4: Laboratoire de Chimie Théorique, Université Paris Sud, 91405 Orsay Cedex, France

In a large number of cases, the dynamics of complex reaction mechanisms may proceed by a series of elementary processes, induced often by a fast reaction step, followed by relaxation or reorganisation of the molecular system. A good description of these elementary processes is thus determinant in understanding such complex mechanisms, as those involved in the action of radiation on biomolecules, or more generally on reactions involving systems of biological interest. Although biological reactions occur mainly in a solvent, studies in the gas phase exhibit the specific chemistry of free species and are often the only way to provide precise data and thermodynamic properties essential for modelizations.

Electron transfer is an important process in physics, chemistry and biochemistry. In particular, charge transfer involving multiply charged ions in collision with atomic or molecular targets are determinant processes in controlled thermonuclear fusion research and astrophysical plasmas. In such processes, an electron is generally captured in an excited state of the ion, followed by line emission. The observation of line intensities provides important information on the electron temperature, density and spacial distributions in the emitting region of the plasma.

From a theoretical point of view, the study of these processes for collision energies from eV to keV is developed in the molecular framework and requires the determination of potential energy surfaces of the different ground and excited states involved in the process , as well as the non-adiabatic couplings between these levels. The dynamical treatment requires then different approaches with regard to the collisional energy range of the process. A semi-classical method is currently used at keV energies and may be extended easily to ion/molecule systems, but the description of very low-velocity processes requires a complete quantum mechanical treatment of the dynamics of both electrons and nuclei. The first approach extensively used is the resolution of the stationary close-coupling equations, but we have analyzed recently on the Si^{4+} + He system, the efficiency of a time-dependent wave packet method [1,2] which provides a clear and physical insight into the dynamics of the processes and may be particularly interesting for polyatomic systems since it allows the possibility of developing a fully quantal mechanical treatment for some degrees of freedom, the other ones being treated classically. This approach is particularly interesting for systems of increasing complexity. In particular many important steps in biological dynamics imply few degrees of freedom imbedded in a bath of inactive coordinates for which a hierarchy can be designed.

As a first example, we have undertaken, in relation with photodissociation experiments [3], the study of competitive dissociation of C-Cl and C-Br bonds in bromacetylchloride Br-CH_2-COCl. The dissociation is induced by an electronic excitation and is shown experimentally to lead preferentially to C-Cl breaking, although the C-Br bond is thermodynamically weaker. This result is in disagreement with statistical theories, as the branching ratio depends not only on the relative height of the corresponding barriers, but also on non-adiabatic transitions arising from interactions between the different excited states. The

effect depends on the distance between the C=O and C-X chromophores and on the conformation of the molecule.

References

[1] N. Vaeck, M.C. Bacchus-Montabonel, E. Baloïtcha, M. Desouter-Lecomte, *Phys. Rev. A* **63**, 042704 (2001).

[2] E. Baloïtcha, M. Desouter-Lecomte, M.C. Bacchus-Montabonel, N. Vaeck, *J. Chem. Phys.* **114**, 8741 (2001).

[3] P.W. Kash, G. Waschewsky, L. Butler, M. Francl, *J. Chem. Phys.* **99**, 4479 (1993).

Biological effects of ionizing radiation: Impact of protons on biomolecules

B. Coupier, B. Farizon, M. Farizon, M.J. Gaillard, F. Gobet

Institut de Physique Nucléaire de Lyon,
IN2P3-CNRS et Université Claude Bernard,
43 boulevard du 11 Novembre 1918, F-69622 Villeurbanne Cedex, France

M. Carré,

Laboratoire de Spectrométrie Ionique et Moléculaire,
CNRS UMR 5579 et Université Claude Bernard,
43 boulevard du 11 Novembre 1918, F-69622 Villeurbanne Cedex, France

G. Hanel, M. Lezius, P. Scheier, T.D. Märk

Institut für Ionenphysik, Leopold Franzens Universität
Technikerstr.25
A-6020 Innsbruck, Austria

S. Ouaskit

Laboratoire de Physique de la matière condensée, Faculté des sciences Ben M'sik
Casablanca, Maroc

N.V. de Castro Faria, G. Jalbert

Université Fédérale de Rio de Janeiro
Rio de Janeiro, Bresil

Abstract

Today it is recognized that radiation damage in bio-molecules, in particular strand breaking in the DNA, is not only the result of a single interaction of the primary ionization projectile with the molecules involved, but also due to the simultaneous and consecutive action of the primary and the secondary species, including also radicals (for instance oxygen) that are produced by destruction of the water molecules surrounding the DNA. A detailed knowledge of the ionization process is a must for a full understanding of radiation damage on a microscopic level .

The research program that we developed at the Institut de Physique Nucléaire de Lyon is focused on the study of swift proton impact ionization of biomolecules in the gas phase and of mixed clusters (DNA or RNA basis and water molecules). The proton energy range (30-150 kV) explored corresponds to a range where proton beam action in living matter is known to be maximum (Bragg peak range). This program is also related to our previous results [1-3] on statistical description of collision induced fragmentation of molecular clusters. Indeed, the relaxation of these highly excited molecular complex systems is also of fundamental interest.

Preliminary experiments are devoted to the measurement of fragmentation cross sections of a target molecule in coincidence with the post-collision charge state of the projectile. Therefore, we are able for the first time to separate the direct ionization and the ionization via electron capture by the projectile. This work give new insights on ionization and charge exchange processes in the interaction of protons and neutral hydrogen atoms with water and biomolecules such as DNA or RNA bases.

We will present experimental results [4] for proton ionization of water molecules based on a novel event by event analysis of the different ions produced (and lost). We are able to obtain mass analyzed product ion signals (e.g., H_2O^+, OH^+, O^+, O^{++}, H^+, and also negative ions) in coincidence with the charge-analyzed projectile, i.e., either being H^+ or after single electron capture during the ionization event neutral H or H^- after double electron capture. After proper calibration we are thus able to determine a complete set of cross sections for the ionization of a molecular target by protons (20-150 keV) including the total and the partial cross sections and in addition also the direct ionization and the electron capture cross sections.

This work has been extended in two directions: Similar measurements have been performed on the one hand for ionization of water by swift neutral atoms, on the other hand for proton ionization of uracil molecules (RNA Base) of which we will present preliminary results.

Acknowledgement

This work is supported by the Amadeus program of the French and Austrian governments

References

[1] B. Farizon, M. Farizon, M.J. Gaillard, F. Gobet, M. Carré, J.P. Buchet, P. Scheier , and T.D. Märk, *Phys. Rev. Lett.* **81** (1998) 4108

[2] F. Gobet, B. Farizon, M. Farizon, M.J. Gaillard, J.P. Buchet, M. Carré, P. Scheier, and T.D. Märk, *Phys. Rev. A* **63** (2001) 033202

[3] F. Gobet, B. Farizon, M. Farizon, M.J. Gaillard, J.P. Buchet, M. Carré, and T.D. Märk, *Phys. Rev. Lett.* **87** (2001) 203401

[4] F. Gobet, B. Farizon, M. Farizon, M.J. Gaillard, M. Carré, M. Lezius, P. Scheier and T.D. Märk, *Phys. Rev. Lett.* **86** (2001) 3751

Non-Covalent Interactions and H/D Exchange of Protonated Peptides and Peptide Clusters

Chava Lifshitz

Department of Physical Chemistry and The Farkas Center for Light Induced Processes, The Hebrew University of Jerusalem, Jerusalem 91904, Israel

Flow-tube mass spectrometry as a technique to measure positive ion-molecule reactions in the gas phase has been reviewed recently [1]. It is an excellent and versatile method for studying chemical kinetics over a wide temperature and energy range. It has been applied to a wide variety of chemical systems – ionospheric reactions, interstellar chemistry, electron transfer, proton transfer, organometallic ion chemistry, and fullerene ion chemistry are just a few examples. There is increasing interest in recent years in anhydrous protein and peptide ions [2]. Electrospray ionization (ESI) [3] provides a very efficient way of introducing singly protonated and multiply protonated peptide ions into the gas phase. We have employed the combination of ESI and flow-tube mass spectrometry in kinetic studies of reactions of small [4-6] and medium sized [7] protonated peptides with ammonia and methanol. Ion/molecule reactions were conducted under carrier gas pressures of several tenths of a torr. We have observed the formation of collisionally stabilized complexes of GLY_2H^+ with NH_3, methanol and a series of amines and studied their formation kinetics. In a study of H/D exchange with ND_3 we have monitored for the first time the collision complexes corresponding to the consecutive H/D exchanges of the five labile hydrogens in protonated diglycine. The formation kinetics, multi-collision-induced dissociation and H/D exchange characteristics were studied for the protonated betaine/ammonia complex that has partial zwitterionic character [8].

Conformational properties of biomolecules in solution are said to be preserved during the process of ESI. Conformational changes in proteins are probed by hydrogen-exchange ESI mass spectrometry. The generally held idea has been that compact structures protect some labile hydrogen atoms from H/D exchange in the gas phase. The interpretation of H/D exchange experiments requires knowledge of the reaction mechanisms involved. Many studies of H/D exchange between protonated peptides and deuterated solvent molecules were performed. ND_3 was found to be the most efficient reagent studied for promoting H/D exchange. Most of these studies were carried out at very low ion source pressures of $10^{-7} – 10^{-5}$ torr in FT-ICR mass spectrometers.

We studied reactions of the doubly-protonated nonapeptide bradykinin and the octapeptide *des*-Arg^9 bradykinin with CH_3OD and ND_3, respectively, by using flow-tube mass spectrometry. Deconvolution of the experimental mass spectral data followed by simulation of the kinetic data by solution of differential equations led to sets of apparent and site-specific rate constants. On a time scale of several milliseconds, bradykinin was observed to undergo with ND_3 three fast H/D exchanges and one slow exchange. Three equivalent exchanges were observed with CH_3OD that were nearly two orders of magnitude slower than the ND_3 reactions. Up to six exchanges of hydrogen were observed for the reaction of *des*-Arg^9 bradykinin with ND_3. The more efficient exchange of *des*-Arg^9 bradykinin was accompanied by formation of collisionally stabilized complexes between doubly-protonated *des*-Arg^9 bradykinin and ND_3 at a He carrier gas pressure of about 0.2 torr.

The above results led to the conclusion that complexation of doubly-protonated bradykinin by ND_3 is prevented by its tightly folded structure and this in turn prevents H/D exchange of the amide hydrogens of bradykinin. The additional H/D exchanges observed in the case of

doubly-protonated *des*-Arg^9 bradykinin are made possible by complexation of its less compact structure via hydrogen bonded intermediates that promote H/D exchange of amide hydrogens.

Among other peptides we have also studied the protonated pentapeptide leucine enkephalin, Tyr-Gly-Gly-Phe-Leu (YGGFL) [9]. On a time scale of several milliseconds, leucine enkephalin undergoes with ND_3 four fast H/D exchanges and one slow exchange. Evidence was presented for the presence of two noninterconverting ion populations with different reactivities however the source of these two populations was not uniquely identified. We have also reported on the discovery [10] in the reaction system, of the doubly protonated dimer of leucine enkephalin, through its reduced reactivity in the H/D exchange reaction with ND_3 compared to the singly protonated monomer.

The electrospray ionization/fast flow apparatus is shown schematically in Figure 1. It consists of a SIFT apparatus that we have constructed several years ago and modified to work with an electrospray (ES) source connected directly to the flow tube. It consists of a flow reactor that is 123 cm in length and an inner diameter of 74 mm. A neutral reagent is introduced into the flow tube through either one of two ring inlets. Tylan mass flow controllers define the flow rate of the neutral reactant into the flow tube. The quadrupole mass analyzer (652601 ABB EXTREL) is housed in a differentially pumped chamber that is separated from the flow tube by a nose cone (NC) skimmer with a 1.0 mm sampling orifice. A small NC voltage is used for focusing ions into the analysis quadrupole. Helium buffer gas enters the flow tube at the upstream end near an electron impact ion source through another Tylan flow controller. It is pumped through the tube by a Roots blower with flow velocities of 2000-4500 cm s^{-1} leading to typical flow tube pressures ranging from 0.15 to 0.4 torr and reaction times of several ms.

The electrospray ion source was designed as follows. A capillary tube serves as the interface between the electrospray and the helium flow reactor. Stainless-steel tubes 15 cm in length and 0.05 cm i.d. are employed. The entire assembly is inserted into the flow tube at a distance of ~ 96 cm from the sampling orifice, 135° to the direction of the helium flow, through an 'O'-ring type vacuum fitting. A capillary tube of 0.05cm i.d. introduces an air leak into the flow tube with a pressure of 0.07 Torr and a flow rate of 1.3 l/min (STP); these numbers have to be added to the helium pressure and helium flow rate when calculating rate constants. Ions are electrosprayed ~10 mm through ambient air into the grounded capillary tube from a stainless steel syringe needle biased at 5 kV DC. Dilute solutions of the analyte of interest in a polar solvent are delivered to the electrospray needle at flow rates of 3.3 μL min^{-1} from a 5000 μL syringe mounted on a model 100 KD Scientific Syringe Pump. The temperature of the capillary tube as well as of the flow tube is in the range of 22-30 C.

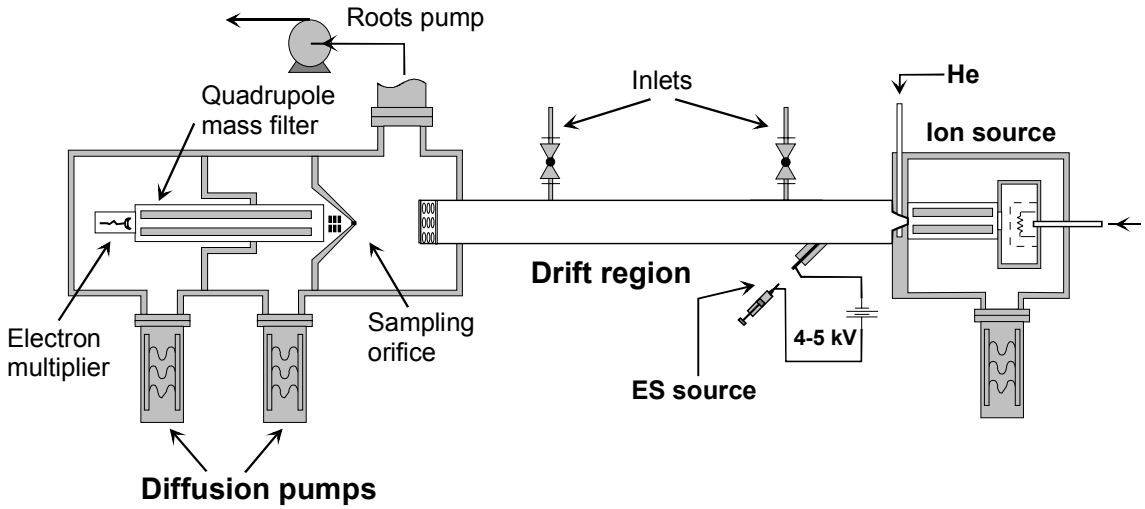

Figure 1

References

[1] Böhme, D. K. *Int. J. Mass Spectrom.* 2000, **200**, 97.
[2] Hoaglund-Hyzer, C. S.; Counterman, A. E.; Clemmer, D. E. *Chem. Rev.* 1999, **99**, 3037.
[3] Fenn, J. B.; Mann, M.; Meng, C. K.; Wong, S. F.; Whitehouse, C. M. *Mass Spectrom. Rev.* 1990, **9**, 37.
[4] Koster, G.; Soskin, M.; Peres, M.; Lifshitz, C. *Int. J. Mass Spectrom.* 1998, **179/180**, 165.
[5] Koster, G.; Lifshitz, C. *Int. J. Mass Spectrom.* 1999, **182/183***,* 213.
[6] Koster, G; Lifshitz, C. *Int. J. Mass Spectrom.* 2000, **195/196***,* 11.
[7] E. Levy-Seri, G. Koster, A. Kogan, K. Gutman, B. G. Reuben, C. Lifshitz., *J. Phys. Chem. A*, **105** (2001) 5552.
[8] C. Zhu and C. Lifshitz, *Chem. Phys. Lett.* **320** (2000) 513
[9] P. Ustyuzhanin, A. Kogan, B. G. Reuben, C. Lifshitz, *Int. J. Chem. Kin.*, **33** (2001) 707.
[10] A. Kogan, P. Ustyuzhanin, B. G. Reuben, C. Lifshitz, *Int. J. Mass Spectrom.* In press

Temperature dependencies in dissociative electron attachment to chloro-bromo methanes

I. Ippoly, V. Foltin, M. Stano and Š. Matejčík

Department of Plasma Physics, Comenius University, Mlynska dolina F2, 84248 Bratislava

I. Introduction

Electron attachment reactions play important role in various fields of chemistry and physics and in a large number of technological applications (gas dielectrics in high-voltage devices, certain types of discharges and plasma) [1]. Due to this, EA reactions have attracted scientific attention and have been studied in many experiments. Previous EA studies to large number of molecules demonstrated that the electron attachment reactions depend strongly on the kinetic energy of electrons. In many cases EA to the molecules is strong enhanced by heating the attaching gas to higher gas temperatures (T_g)[2].

The present work is devoted to the study of the gas temperature effect on the dissociative electron attachment (DEA) to the chloro-bromo-methanes:

$e + CH_2BrCl \rightleftarrows (CH_2BrCl)^{-*}$	$\rightarrow Cl^- + CH_2Br$	R1
	$\rightarrow Br^- + CH_2Cl$	R1b
$e + CHCl_2Br \rightleftarrows (CHCl_2Br)^{-*}$	$\rightarrow Cl^- + CHClBr$	R2a
	$\rightarrow Br^- + CHCl_2$	R2b
$e + CHClBr_2 \rightleftarrows (CHClBr_2)^{-*}$	$\rightarrow Cl^- + CHBr_2$	R3a
	$\rightarrow Br^- + CHClBr$	R3b
$e + CFClBr_2 \rightleftarrows (CFClBr_2)^{-*}$	$\rightarrow Cl^- + CFBr_2$	R4a
	$\rightarrow Br^- + CFClBr$	R4b
$e + CCl_3Br \rightleftarrows (CCl_3Br)^{-*}$	$\rightarrow Cl^- + CCl_2Br$	R5a
	$\rightarrow Br^- + CCl_3$	R5b

This study has been performed in the electron energy range from 0 to 2 eV and in the gas temperature range from about 300 K to about 500 K using a new crossed electron-molecular beams apparatus with a temperature regulated, effusive molecular beam source.

The gas temperature studies of DEA to these molecules are of fundamental interest. The DEA reactions R1a-R5b are exothermic reactions, with a competition between two separate reaction channels (Cl^- and Br^-). For some of these molecules the overall DEA rate coefficients have been measured by Sunagawa and Shimamori [3] and the temperature dependencies of the rate coefficients for particular reaction channels have been measured by Smith and Spanel [4]. In present contribution, the distribution of the reaction products into these two channels has been studied as a function of the electron energy and the gas temperature.

II. Experiment

The present study has been carried out using a new high-resolution electron-molecular beam apparatus [5]. The electron beam formed by a Trochoidal Electron Monochromator (TEM) is perpendicular crossed by a molecular beam formed by an Effusive Molecular Beam Source (EMBS). The negative ions produced in the reaction chamber are extracted by a weak electric field from the reaction chamber and focused into the entrance of a Quadrupole Mass Spectrometer (QMS). The intensity of a selected negative ion is then measured as a function of the electron energy E and the gas temperature T_g. The electron energy distribution function

of the electrons in the electron beam (measured as a Full With at Half Maximum FWHM) of around 70 meV has been used in the present experiment. The EMBS consists of a heatable stainless steel container, gas inlet system, heaters and a pair of thermocouples. The pressure in EMBS is measured using an absolute pressure gauge (MKS Barratron, pressure range 0-7Pa). The gas is effusing from the EMBS trough a single channel (5mm long, 0.5mm diameter). The molecular beam is formed by the effusion of the molecules trough the channel. The EMBS was resistively heated (temperature range 300 K– 500 K). The temperature of the EMBS was measured using a pair of thermocouples (chromel, alumel). The gas inlet system of the EMBS was working at higher pressure (typically 10^5-10^2Pa). The reacting gas was introduced to the EMBS using a precise diaphragm-regulating valve, reducing the gas pressure to 0.1-7 Pa. For the temperature dependent studies it is important to known, the variation of the gas number density in the molecular beam with the gas temperature. The number density of the molecule in the molecular beam is decreasing with the increasing T_g:

$$n_o \sim T_g^{-0.5} \quad (1)$$

providing the gas flow through the EMBS is constant [5]. If the cross section for a DEA reaction does not depend on T_g, the ion signal should decrease with T_g as the $T_g^{-0.5}$.

III. Results

In the Figures 1a-5a are presented the measured ion yields for the reactions R1-R5 as the functions of the kinetic energy of the electrons in the electron energy range 0-1.75 eV. The Cl^- and Br^- ions yields have been measured at the gas temperatures indicated in the graph. The intensities of Cl^- and Br^- ions measured at the zero electron energy as functions of the gas temperature are shown in the Figures 1b-5b.

In the case of the molecule CH_2ClBr (Fig.1a, 1b), the Br^- ion is the dominant reaction product in the whole electron energy range from 0 to 1.75 eV. The ion yield for Br^- has a peak at 0 eV and a shoulder between 100 meV and 500 meV indicating a second resonance in this region. The ion yield for Cl^- channel has a peak at 0 eV and then signal decreases monotonically in the whole electron energy range. With the increasing gas temperature the Br^- ion signal at 0 eV electron energy is increasing and is becoming even more dominant product (Fig. 1b). The intensity of the Cl^- ion is decreasing with the increasing gas temperature. The $T_g^{-0.5}$ function in the Figure 1b represents the decrease of the ion signal, due to the decrease of the gas number density of the molecules in the molecular beam with increasing T_g. The Cl^- signal decreases more rapidly with T_g as the $T_g^{-0.5}$ function. This indicates the decrease of the partial cross section at 0 eV with the gas temperature.

The ion yields for Br^- and Cl^- channels (Fig. 2a) for DEA to $CHCl_2Br$ have very similar shape, the maximum at 0 eV and then a monotone decrease in the whole electron energy range from 0 eV up to 1.75 eV. In the electron energy range from 0 eV to about 0.5 eV is the decrease exponential. The Br^- ion is dominant in the whole measured electron energy range. With the increasing gas temperature is Br^- intensity decreasing more rapidly then $T_g^{-0.5}$, indicating the decrease of the partial cross section at 0 eV with increasing T_g. The Cl^- intensity at 0 eV decreases as $T_g^{-0.5}$. This indicates, that the cross section for this reactions channel does not depend on T_g.

The ion yields for DEA to $CHClBr_2$ are presented in the Fig. 3a. The Br^- channel has a maximum at 0 eV and the second resonance is at about 0.5 eV. The Cl^- channel has a maximum at 0 eV and the second resonance is at about 0.6 eV. The Br^- is the dominant product in the whole electron energy range and also at all gas temperature. The Fig. 3b indicates, that the cross section for the Br^- channel at 0 eV is constant with T_g and that the cross section for Cl^- channel is increasing with increasing T_g.

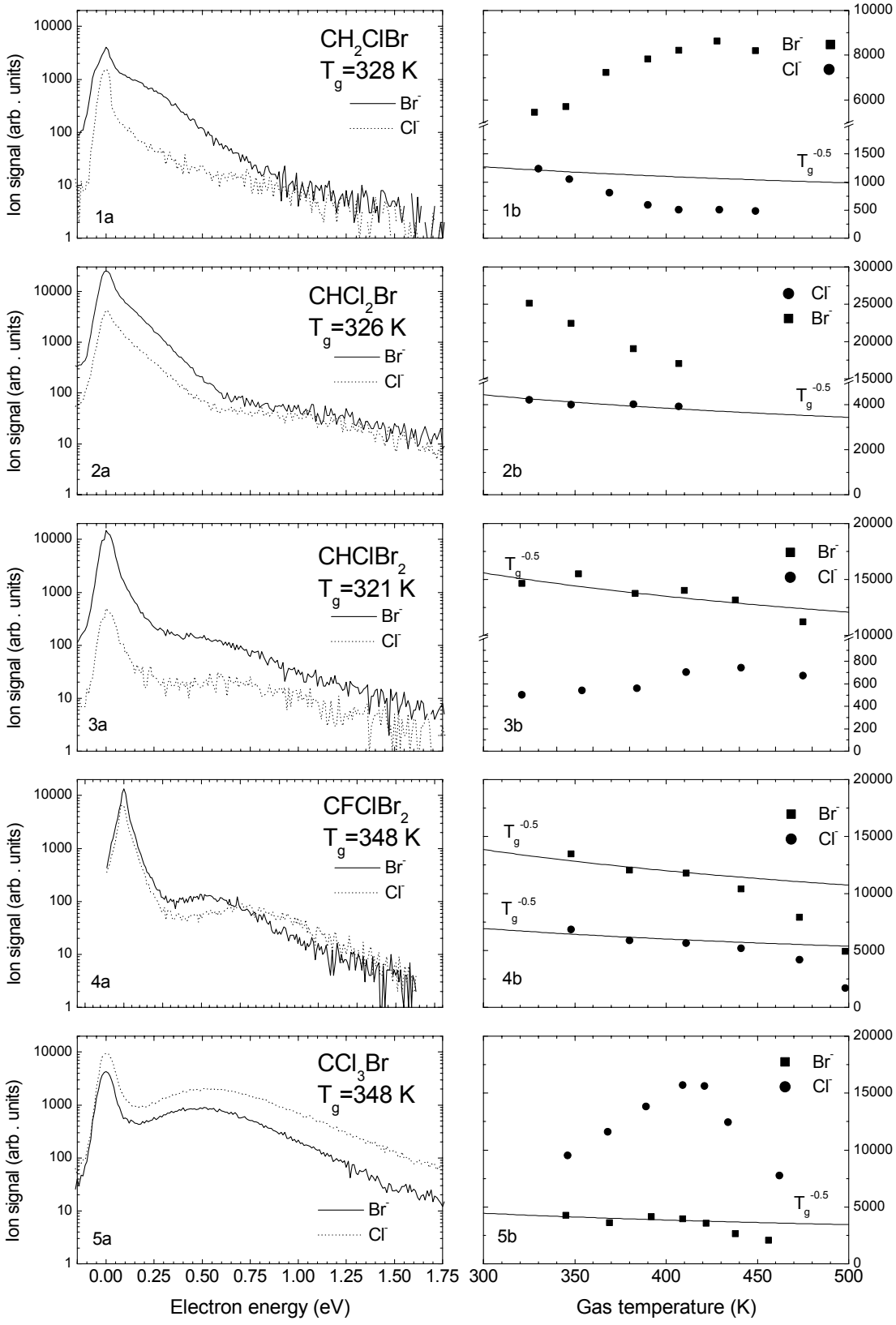

Figures 1a-5b

The ion yields for DEA to $CFClBr_2$ are presented in the Fig. 4a. For the Br^- reaction channel the first peak can be found at 0 eV and the second resonance at about 0.6 eV. The ion yield for Cl^- reaction channel has first peak at 0 eV and the second at about 0.8 eV. At the electron energies below 0.75 eV Br^- is the dominant ion and above 0.75 eV Cl^- is the dominant ion. The temperature dependencies of the 0 eV peaks show monotone ($T_g^{-0.5}$) decrease of the Br^- and Cl^- signals with increasing T_g in the gas temperature range form 348 K up to 440 K. This indicates, that the cross sections at low electron energies for both reaction channels do not depend on T_g. At the gas temperatures above 440 K the decrease of the Cl^- and Br^- signals is stronger then $T_g^{-0.5}$. This is most probably due to thermal decomposition of $CFClBr_2$. Due to thermal decomposition of the molecules in the EMBS, the number density of the molecules in the molecular beam decreases more rapidly then predicted by (1) and therefore also ion signals are decreasing. Similar effects have been observed in [5] for other molecules.

In the reactions R1-R4 dominant product of the reactions has been found Br^-. In the case of CCl_3Br is the situation different. At the gas temperatures above 348 K is Cl^- ion the dominant product in the whole electron energy range. Spanel et al. [6] observed that at 297 K the dominant ion is Br^-, but in the present experiment it was not possible to measure this reaction at such low temperature. The Br^- ion yield curve has two peaks, the first one at 0 eV and the second one at about 0.5 eV. The Cl^- ion yield has also two peaks, the first one at 0 eV and the second at about 0.6 eV. Spanel et al. observed the second peaks at slightly different electron energies. With the increasing gas temperature the Cl^- signal at 0 eV is increasing rapidly, but at the gas temperature above 420 K strong decrease of the signal is observed. This decrease is attributed to the thermal decomposition of CCl_3Br molecule in the EMBS. This effect can be observed also for the Br^- ion. The Br^- signal is decreasing with the increasing gas temperature according to $T_g^{-0.5}$ law (indicates temperature independent cross section), but at the gas temperatures above 420 K strong decrease of the Br^- signal is observed, this decrease is attributed to thermal decomposition.

Acknowledgment:

This work was partially supported by the German Volkswagen Foundation and by the Slovak Grant Agency VEGA, project Nr. 1/8313/01.

References

[1] L. G. Christophorou (Ed.), Electron-Molecules Interactions and Their Applications, Academic, Orlando, 1984.
[2] L.G. Christophorou, J. K. Olthoff, *Adv. At. Mol. Opt. Phys.* **44** (1999) 155
[3] T. Sunagawa, H. Shimamori, *J. Chem. Phys.*, **107** (1997) 7876
[4] P. Spanel, D. Smith, *Int. J. Mass. Spect.*, **205** (2001) 243
[5] S. Matejcik, V. Foltin, M. Stano, J.D. Skalny, *Int. J. Mass. Spect.*, sent for publication
[6] P. Spanel, D. Smith, S. Matejcik, A. Kindler and T. D. Märk *Int. J. Mass. Spect. Ion. Proc.*, **167/168** (1997) 1

Calculation of absolute electron ionization cross sections of DNA bases using the semiclassical DM formalism

Philipp Bernhardt and Herwig Paretzke

GSF − National Research Center for Environment and Health, Institute of Radiation Protection, D−85764, Neuherberg, Germany

Abstract

Electron ionization cross sections for the four DNA bases adenine, cytosine, guanine and thymine have been calculated, using the semiclassical Deutsch−Märk (DM) formalism. For this method a Mullikan population analysis is necessary, which was performed with the Gaussian98 system, using the Hartree Fock method with the 6−31G basis set. Comparison of the first ionization energy revealed good agreement with experimental measurements. The determined cross section of the four bases have common energy dependencies due to the similarity of the bases' chemical structure.

Introduction

To understand the mechanism of radiation induced DNA damage, Monte Carlo track structure simulations are a useful tool to determine energy deposition densities. These simulations require a complete set of cross sections for the respective particles and target materials. Recently developed methods, like the Deutsch−Märk (DM) formalism [1] or the binary−encounter−Bethe (BEB) theory [2] provide an easy access to determine electron ionization cross sections for atoms, molecules, clusters and ions. Here calculations of the electrons ionization cross sections for the four DNA bases adenine, cytosine, guanine and thymine are presented, using the DM formalism.

Methods

The semiclassical Deutsch−Märk (DM) formalism is fully described in [1,3−9]. Here a short outline in the case of molecules is given:

The molecular orbitals j first must be expressed in terms of the atomic orbitals of the constituent atoms. This can be done by a Mullikan population analysis.

The total ionization cross section is then calculated by:

$$\sigma = \sum_j' g_j \pi (r_j)^2 \xi_j f(E/E_j) \quad .$$

g_j is called the weighting factor and is dependent on the constituent atomic subshells and binding energy E_j of the molecular orbital. $(r_j)^2$ represents the mean square radius of the constituent atomic subshells and ξ_j gives the effective number of electrons in the atomic subshells according to the Mullikan analysis. $f(E/E_j)$ contains the dependence of the ionization cross section on the energy E of the incoming electron. All parameters for the DM formalism were taken from the actual DM data set [1].

The structures of the four bases adenine, cytosine, guanine and thymine were downloaded from Klotho [10] and can be seen in figure 1. The Mullikan population analysis for these four structures was performed with the Gaussian98 system. Hartree−Fock (HF) theory was used together the 6−31G basis set for the single point calculations. Applying more sophisticated basis sets like 6−311G** did not have a significant influence on the binding energies of the molecular orbitals.

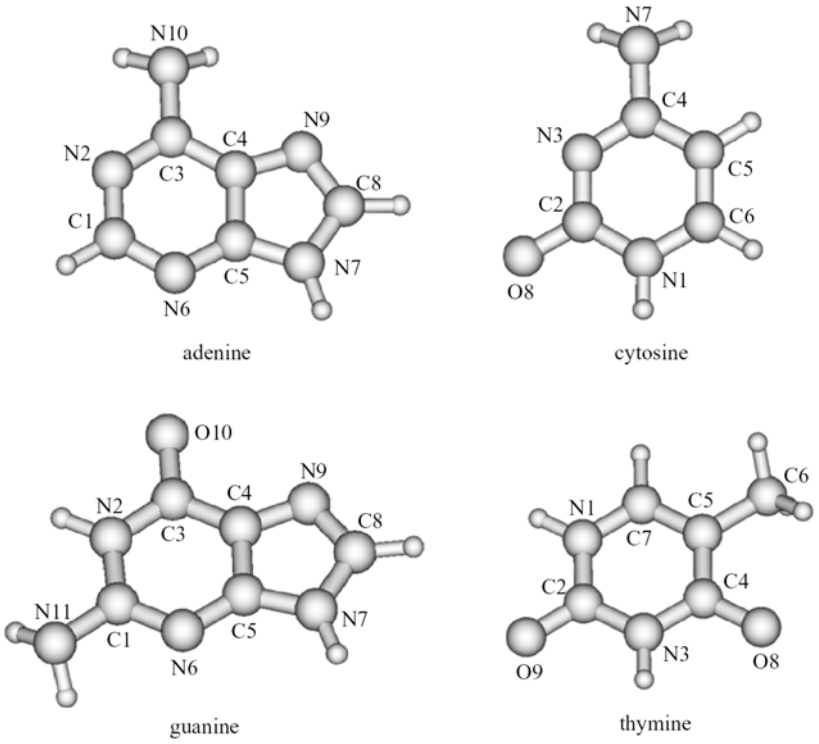

Figure 1: The chemical structures of the four DNA bases

Results and Discussion

Table 1 gives a comparison between the calculated binding energy of the HOMO (highest occupied molecular orbital) and measurements of the ionization energies, which references were taken from [11] for the four bases.

	adenine	**cytosine**	**guanine**	**thymine**
this work	8.67 eV	9.12 eV	8.13 eV	9.57 eV
measurements	8.3 ± 0.1 eV [12]	8.45 eV [17]	7.85 eV [17]	9.0 ± 0.1eV [12]
	8.9 ± 0.1 eV [13]	9.0 ± 0.1 eV [12]	8.0 ± 0.2 eV [12]	9.4 ± 0.1 eV [13]
	8.48 eV [14]	8.9 ± 0.2 eV [13]	8.24 ± 0.03 eV [16]	9.20 eV [17]
	8.48 eV [15]	8.94 ± 0.03 eV [16]		9.02 eV [18]
	8.44 ± 0.03 eV [16]			9.14 ± 0.03 eV [16]

Table 1: Comparison between the binding energy of the HOMO of the four DNA bases with measurements of the ionization energy.

The values from the ab−initio calculations deliver values slightly above the measurements. This is a consequence of the HF algorithm, which generally overestimates binding energies due to the neglecting of the correlation energy of the electrons.

In table 2 Mullikan representation of the 4 highest occupied molecular orbitals for adenine is listed, together with parameters necessary for the calculation of the electron cross sections. Only atomic shells with a certain amount of effective number of electrons are presented, which explains, that the sum of the number of electrons for every MO is lower than 2. The valence orbitals are quite delocalized.

g^j_{nl}	$\xi^j_{A,nl}$	$r_{A,nl}(10^{-11}$ m)	E_j (eV)	atom A	nl
2.583	0.196	6.443	11.62	C4	2p
2.583	0.565	5.236		N7	2p
2.583	0.615	5.236		N9	2p
2.583	0.452	5.236		N10	2p
2.753	0.624	5.236	10.90	N2	2p
2.753	0.121	6.443		C4	2p
2.753	0.679	5.236		N6	2p
2.753	0.159	5.236		N9	2p
2.935	0.101	6.443	10.22	C1	2p
2.935	0.714	5.236		N2	2p
2.935	0.261	6.443		C4	2p
2.935	0.280	6.443		C5	2p
2.935	0.202	5.236		N6	2p
2.935	0.211	5.236		N7	2p
2.935	0.129	6.443		C8	2p
3.459	0.153	6.443	8.67	C1	2p
3.459	0.145	6.443		C3	2p
3.459	0.377	6.443		C4	2p
3.459	0.106	6.443		C5	2p
3.459	0.326	5.236		N6	2p
3.459	0.266	6.443		C8	2p
3.459	0.170	5.236		N9	2p
3.459	0.360	5.236		N10	2p

Table 2: Results of the Mullikan analysis for adenine for the 4 highest occupied molecular orbitals, showing the weighting factor g^j_{nl}, the effective number of electrons $\xi^j_{A,nl}$ in the atomic subshell A,nl, the root mean square radius $r_{A,nl}$ and the ionization energy of the molecular orbital j. Further explanations are provided in the text.

Finally the resulting absolute electron cross sections per base molecule in dependence on the incoming electron energy can be seen in figure 2. The bases consist of the same type of atoms and binding mechanism, which leads to a large similarity of the cross section. The maximum is around 80 eV. Distinctions are mainly caused by the variant number of atoms.

Conclusion

The semiclassical DM formalism was applied to calculate electron cross sections for the four DNA bases. Further work will be invested to calculate electron ionization cross sections for the DNA backbone. These data are useful for detailed Monte Carlo track structure simulations.

Acknowledgement

We thank Mr. Märk, Mr. Probst and Mr. Deutsch, for helpful discussions and support.

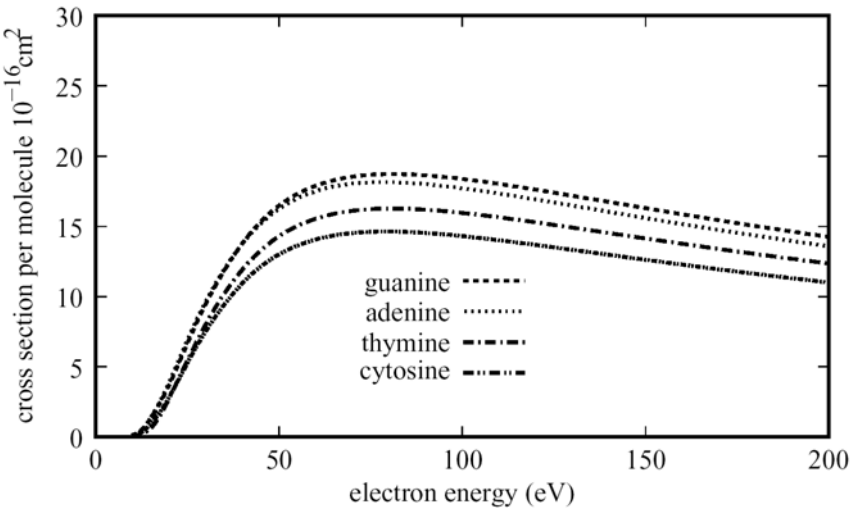

Figure 2: Electron ionization cross sections for the four DNA bases in dependence on the incoming electron energy

References

[1] H. Deutsch, K. Becker, S. Matt and T.D. Märk, *Int. J. Mass Spec.* **197**, 37−69 (2000)
[2] Y.K. Kim, W. Hwang, N.M. Weinberger, M.A. Ali and M.E. Rudd, *J. Chem. Phys.* **106**, 1026 (1997)
[3] D. Margreiter, H. Deutsch, M. Schmidt and T.D. Märk, *Int. J. Mass. Spec. Ion. Proc.* **100**, 157−176 (1990)
[4] D. Margreiter, H. Deutsch and T.D. Märk, *Int. J. Mass Spec. Ion. Proc.* **139**, 127−139 (1994)
[5] H. Deutsch, J. Pittner, V. Bonacic−Koutecky, K. Becker, S. Matt and T.D. Märk, *J. Chem. Phys.* **111**, 1964−1971 (1999)
[6] H. Deutsch, K. Becker, R.K. Janev, M. Probst and T.D. Märk, *J. Phys. B: At. Mol. Opt. Phys.* **33**, L865−L872 (2000)
[7] M. Probst, H. Deutsch, K. Becker and T.D. Märk, *Int. J. Mass. Spec.* **206**, 13−25 (2001)
[8] H. Deutsch, K. Hilpert, K. Becker, M. Probst and T.D. Märk, *J. App. Phys.* **89**, 1915−1921 (2001)
[9] U. Onthong, H. Deutsch, K. Becker, S. Matt, M. Probst and T.D. Märk, *Int. J. Mass Spec.*, in print 2001
[10] Klotho: Biochemical Compounds Declarative Database, (http://www.ibc.wustl.edu/moirai/klotho)
[11] P.J. Linstrom and W.G. Mallard, Eds., NIST Chemistry WebBook, NIST Standard Reference Database Number 69, July 2001, NIST, Gaithersburg MD, 20899 (http://webbook.nist.gov)
[12] Verkin, B.I.; Sukodub, L.F.; Yanson, I.K.,Dokl. Akad. Nauk SSSR, 1976, 228, 1452
[13] Lifschitz, C.; Bergmann, E.D.; Pullman, B., Tetrahedron Lett., 1967, 4583
[14] Lin, J.; Yu, C.; Peng, S.; Akiyama, I.; Li, K.; Lee, L.K.; LeBreton, P.R., J. Am. Chem. Soc., 1980, 102, 4627
[15] Peng, S.; Padva, A.; LeBreton, P.R., Proc. Nat. Acad. Sci. U.S.A., 1976, 73, 2966
[16] Hush, N.S.; Cheung, A.S., Chem. Phys. Lett., 1975, 34, 11
[17] Dougherty, D.; Younathan, E.S.; Voll, R.; Abdulnur, S.; McGlynn, S.P., J. Electron Spectrosc. Relat. Phenom., 1978, 13, 379
[18] Lauer, G.; Schafer, W.; Schweig, A., Tetrahedron Lett., 1975, 45, 3939

Interaction of highly monochromatized electrons with molecules of biological relevance

P. Scheier, G. Hanel, B. Gstir, A. Pelc, W. Sailer, H. Drexel, A. Stamatovic and T.D. Märk

Institut für Ionenphysik, Leopold-Franzens Universität, Technikerstr. 25, A-6020 Innsbruck, Austria

The formation of both positively and negatively charged ions has been investigated for the collision of highly monochromatized electrons with molecules such as uracil, formic acid, acetic acid and acetonitrile. The aim of these studies is to understand the basic processes that lead finally to the damage of living cells upon exposure to ionizing radiation (α, β, γ, ions). Sanche and co-workers [1] recently demonstrated that potentially lethal DNA damage (double strand breaks) are not only induced by the primary high energy projectiles. Secondary species of the primary ionizing radiation, like slow electrons with kinetic energies typically below 20 eV, turn out to be even more dangerous leading to substantial cell damage. We have studied on two monochromator instruments the inelastic interaction of low energy electrons with several selected prototypical organic molecules including the RNA base uracil.

Dissociative electron attachment (DEA) to formic acid, acetic acid and acetonitrile was investigated with an electron energy resolution of 50 meV to 100 meV using a trochoidal electron monochromator which has been improved recently [2]. This highly sophisticated ion source is located in an UHV-recipient and heated throughout the experiments with halogen lamps to 370 K to reduce unwanted effects due to surface contaminations. The gaseous samples were introduced through a 20 µm platinum nozzle located closely to the collision chamber as an effusive beam. Clustering of the molecules has not been observed for the presently used pressure parameters. Anions that were formed by the interaction of the low energy electron beam with the molecular beam are focused with a set of electrostatic lenses into a quadrupole mass filter and detected with a channeltron type SEM located off-axis to the quadrupole. For the present setup the neutral target beam and the quadrupole axis are collinear which has the advantage to allow operation of the instrument with practically no extraction field (avoiding secondary effects on the electron beam and the extracted ion beam). Nevertheless, the interaction of extracted anions with other neutral molecules might lead to secondary products. Up to now only autodetached electrons from long living parent anions like $C_2Cl_4^-$ have been identified as a source of such secondary product anions in the extracted ion beam [3]. Results obtained for DEA for these molecules will be discussed and characteristic features (such as H atom loss in DEA) will be compared to the uracil case (see below).

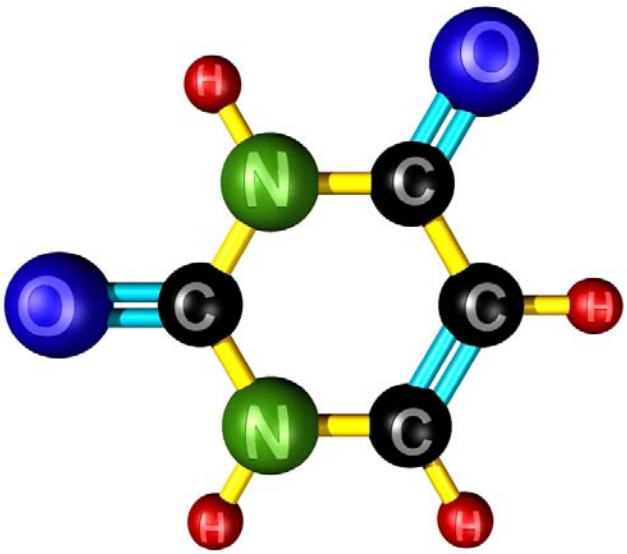

Figure 1: schematic view of uracil

Uracil is one of the four bases in RNA. The others are adenine, guanine, and cytosine. Uracil replaces thymine, which is the fourth base in DNA. Like thymine, uracil always pairs with adenine. Figure 1

is a schematic view of this molecule. When combined with the sugar ribose in a glycosidic linkage, uracil forms a derivative called uridine. There is no uridine in deoxyribonucleic acid (DNA). However, its involvement in the biosynthesis of RNA demonstrates that uracil is important in the translation of genetic information. This molecule can be obtained as a white powder and can be evaporated fragmentation free in a simple oven at about 450 K to 465 K. We performed the experiments on uracil on a crossed beams apparatus equipped with a hemispherical electron monochromator. This instrument has been described in detail previously [4]. It was primarily built in our Innsbruck laboratory for the study of electron-particle interactions under high sensitivity and high energy resolution. The performance of the home built hemispherical electron monochromator has been improved by careful attention to a number of technical details (such as the selection of only one material – stainless steel – frequent bake-out of the instrument and the compensation of the earth's magnetic field with Helmholtz coils). Ions formed in the collision chamber are extracted on line to the neutral beam direction by a weak electric field. Usually, a rather low ion extraction voltage of about 50 mV (corresponding to an electric field strength of about 0.12 V/cm) was used in order to minimize disturbing field effects. The extracted ions are then focused by a system of electrostatic lenses into the entrance of a quadrupole mass spectrometer with a nominal mass range of 2000 amu. The mass selected ions are detected by a channeltron multiplier operated in single ion counting mode.

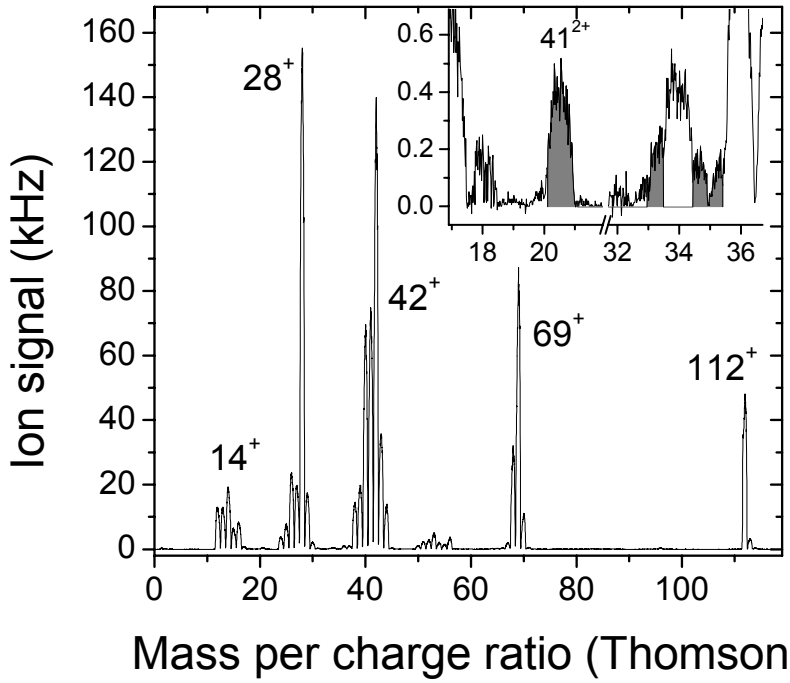

Figure 2: Mass spectrum of the positive ions formed upon electron impact ionization of uracil. Electron energy: 200 eV, oven temperature: 460 K. Shaded peaks in the insert indicate doubly charged fragment ions.

Figure 2 shows a mass spectrum of positively charged product ions that were formed at an electron energy of 200 eV. The quadrupole mass spectrometer was optimized for the H^+. Since the transmission of this type of mass spectrometer is dependent on the mass the relative yield of the heavy ions might be underestimated. On the other hand fragment ions that were formed with high kinetic energy will be extracted from the collision chamber with lower probability. The presence of doubly charged fragment ions (see insert in Figure 2) indicates that Coulomb repulsion of unstable multiply charged intermediate molecular ions might lead to fast singly charged fragment ions that can hardly be collected with the present experimental setup. For positively charged product ions the threshold region of the ion efficiency curves

were measured to a few eV above the expected appearance energy and by fitting a power function of the form

$$f(E) = b + c(E - AE)^p \quad (1)$$

to the data. The parameter b is a possible background signal, AE the appearance energy and, a scaling constant c has a constant value for E≥AE and is set to 0 for E<AE. The exponential factor p is according to Wannier [5] 1.127 in the case of the electron impact ionization of atomic hydrogen. Figure 3 shows a typical example of the threshold region of the ion efficiency curve of the singly charged uracil parent ion and the two most intense fragment ions with a mass per charge ratio of 69 and 42 Thomson, respectively. Table 1 below summarizes the appearance energies that were derived by fitting equation (1) to the experimental data. The errors represent the 68% region of confidence derived from 7 independent measurements. It is interesting to note that the previous value of Lifshitz and coworkers [6] derived for the uracil parent ion (9.82 ± 0.1 eV) using electron impact and a vanishing current method is in good agreement with the present result (9.59 ± 0.06 eV).

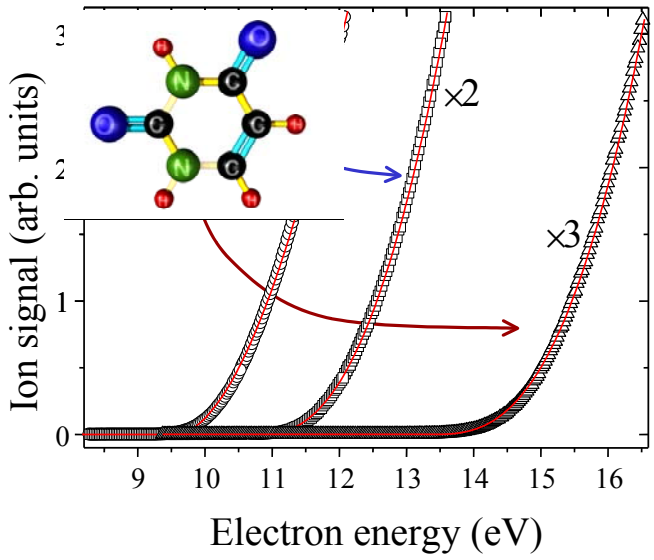

Figure 3: Ion efficiency curves for the uracil parent ion and the two fragment ions $C_3H_3NO^+$ and CNO^+, respectively.

Table 1: Appearance energies derived from the data such as shown in Figure 3 using equation (1).

Symbol	m/z (Thomson)	AE(eV) ± Δ(AE)
○	112	9.59 ± 0.06
□	69	10.87 ± 0.04
Δ	42	13.39 ± 0.02

Using the same hemispherical monochromator instrument it is also possible to study negatively charged product ions with high electron energy resolution. In the present study the following anion fragments of uracil have been identified within our detection limit $(C_4H_3N_2O_2)^-$, OCN^-, $(H_2C_3NO)^-$, CN^-, O^-. The most important result is that the parent anion cannot be observed within our detection efficiency (this has been confirmed by careful measurements of neighboring isotope peaks) in contrast to the situation of bromouracil encountered by Illenberger and coworkers [7] who reported the occurrence of a strong parent anion signal for this molecule. The most intense fragment anion appears on a mass to charge ratio of 111 amu. Mass 111 corresponds to the uracil molecule missing one hydrogen. Moreover, the electron attachment spectrum for this anion exhibits in the energy range from 0 to 3eV a number of well pronounced narrow peaks (see Figure 1 in the abstract by G. Hanel et al. "Low energy electron attachment to the uracil molecule" at the same conference). The zero energy resonance is probably due to an s-wave attachment process.

Acknowledgements.
Work partially supported by the FWF, ÖAW and ÖNB, Wien, Austria. We would also like to thank the French and Austrian governments for supporting this research in the frame of the Amadee program and the European Commission, Brussels.

References

[1] B. Boudaiffa, P. Cloutier, D. Hunting, M.A. Hues and L. Sanche, *Science* **287** (2000) 1658
[2] V. Grill, H. Drexel, W. Sailer, M. Lezius, T.D. Märk, *Int. J. Mass Spectrometry* **205** (2001) 209
[3] H. Drexel, W. Sailer, V. Grill, T.D. Märk and P. Scheier, to be submitted
[4] G. Denifl, D. Muigg, A. Stamatovic and T.D. Märk, *Chem. Phys. Lett.* **288** (1998) 105
[5] G.H. Wannier, *Phys. Rev.* **90** (1953) 817
[6] C. Lifshitz, E.D. Bergmann and B. Pullman, *Tetrahedron Letters* **46** (1967) 4583
[7] H. Abdoul Carime, M.A. Huels, F. Bruning, E. Illenberger and L. Sanche, *J. Chem. Phys.* **113** (2000) 2517

Ion Induced Excitation and Ionization of Uracil

Thomas Schlathölter, Jur de Vries, Ronnie Hoekstra and Reinhard Morgenstern

KVI Atomic Physics, Rijksuniversiteit Groningen, Zernikelaan 25, 9747 AA Groningen, The Netherlands

Introduction

Energy deposition into bio-molecules and their subsequent de-excitation pathways belong to the most fundamental processes occurring in living organisms. In particular the effect of radiation on cellular survival and proliferation is of increasing biological and medical importance. Such radiation damage in biological tissue is to a large extent induced by secondary processes such as the interaction of hyperthermal electrons or ions containing inner-shell vacancies with cellular DNA. To investigate processes of the latter kind, we study the interaction of slow, multiply charged ions (MCI) with the RNA building-block uracil. MCI are particularly interesting because a variable amount of energy and charge can be transferred to the bio-molecule, leaving it vibrationally and/or electronically excited. In the following we present the first experiments on the interaction of MCI with RNA/DNA bases.

Experimental

MCI were extracted from the electron cyclotron resonance ion source (ECRIS) at the atomic physics facility of the KVI. The source can be floated at different voltages between 2 and 20 kV. The ion beam is collimated by two 1 mm diameter diaphragms which are 180 mm apart, with the second diaphragm located 60 mm in front of the collision center.

Uracil, as well as other RNA/DNA bases, can be brought into the gas phase rather easily by means of an oven. The crystalline form is heated to approximately 180 ^{o}C where fragmentation is still negligible but evaporation is already strong. The uracil vapor effuses through a nozzle and two diaphragms and crosses the projectile ion beam in the collision region.

A static electric field of typically several 100 V/cm extracts electrons onto a micro-sphere plate detector, and positive ions through a 5 mm diaphragm into a reflectron type time-of-flight (TOF) mass spectrometer. TOF measurements can be performed in two modes: 1) Continuous beam - the start signal is given either by an electron originating from the collision (electron-ion coincidence mode) or a fragment ion originating from the same collision as the stop-ion (ion-ion coincidence mode). 2) Pulsed MCI beam – the projectile beam is periodically deflected to obtain pulses of 20 ns to 100 ns length which trigger the TOF measurement (chopper-ion coincidence mode). This way all classes of collisions contribute statistically to the spectra and no discrimination is made. The coincidence TOF measurements are performed using a multi-hit TDC with 1ns resolution and virtually unlimited number of coincidences with negligible dead-time. A thorough discussion of the experimental technique is given in [1].

Results and Discussion

Standard mass spectra obtained with a chopped projectile beam are displayed in fig. 1. The upper graph shows results obtained with He^{2+} (v= 0.5 a.u.) projectiles, while for the lower graph O^{6+} (v=0.4 a.u.) ions have been used. Both spectra show very similar features. At m/q=112 the uracil parent cation is found. The next lighter group of peaks has a maximum at m/q=69 and is most probably due to the loss of fragments based on an OCNH group. The next group of peaks has a maximum at m/q=42 and could be due to e.g. OCN^+. Furthermore, we observe a group of peaks between C_2^+ and O_2^+ and another one between C^+ and H_2O^+. At

small *m/q* also contributions of H^+ and H_2^+ are observed. We note, that the peaks from H^+, H_2^+, H_2O^+, N_2^+ or O_2^+ may be partly due to interaction of the projectile ions with residual gas molecules.

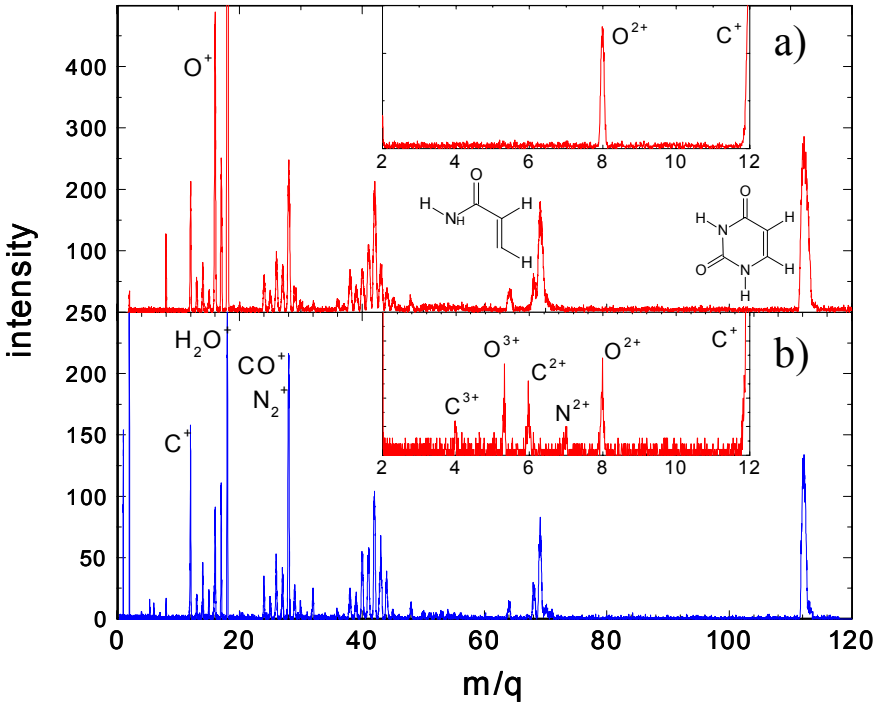

Figure 1 Mass spectra of the products from He^{2+} (a) and O^{6+} (b) collisions with uracil. The inset shows a zoom in the low mass region.

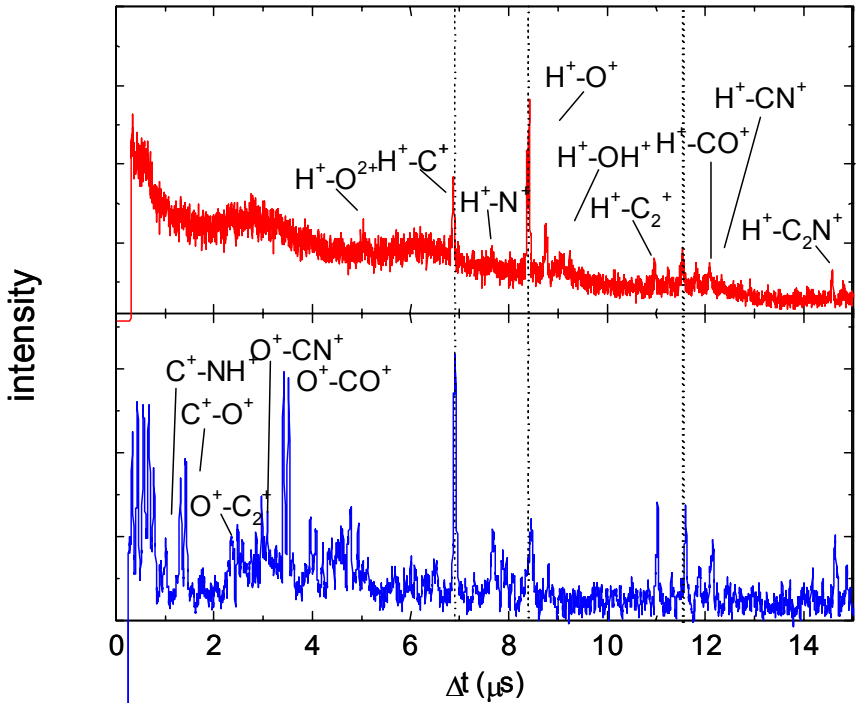

Figure 2 Fragment ion-fragment ion coincidence spectra of the products from He^{2+} (a) and O^{6+} (b) collisions with uracil.

The characteristic features of the spectra differ only in details when comparing He^{2+} and O^{6+} projectile-ions. On the first glance, this suggests that very similar processes are active

during and after the collision process, in strong contrast to the case of e.g. fullerenes. To address this question in more detail, we also measured coincidence TOF spectra.
These spectra are displayed in fig. 2 for the same conditions as fig. 1. Note that the labels on the different peaks give the most likely possibilities of coincidence pairs. In some cases, also other assignments might contribute to the same peak.
However, large differences between the He^{2+} and the O^{6+} cases are obvious. For He^{2+} (fig. 2a) no distinct peaks are visible with a Δt smaller than 5 µs. A thorough analysis of the peaks at larger Δt reveals that in this case most probably all peaks are due to protons.
No coincidences between fragments with larger mass are observed. This changes when looking at the O^{6+} data (fig. 2b). Here, a multitude of peaks is found at low Δt which are mainly due to coincidences between C^+ or O^+ and other atomic and molecuar cations. Furthermore just as for He^{2+} also the proton coincidences are present, although with different relative intensities.

The reasons for the pronounced differences are not fully understood, yet. The average charge on the target molecule is certainly higher in case of O^{6+} projectiles, leading to more or higher charged fragments. However, from what is known from the fullerene studies, also for the case of doubly charged projectiles a removal of on average more than 2 electrons is expected [2,3,4]. Close collisions involve small impact parameters and should therefore be more violent than those with higher charged projectiles.

More light can be shed on this question by looking at electron-ion coincidence TOF spectra as displayed in fig. 3. In this mode, all single electron capture events are suppressed, since in those events no electron is emitted. This leads to a strong reduction of residual gas contributions and an increase in intensity for peaks due to multiple electron capture. In the electron-ion spectrum multiply charged fragments up to C^{3+} and O^{3+} are observed with high relative intensity. Not shown here are the results for He^{2+} projectiles, where these peaks are still not observed. The presence of a strong contribution of the multiply charged species in the spectra suggests that in one event several ions are produced and that the intermediate uracil-ion formed during the collision most probably breaks apart due to a Coulomb explosion mechanism.

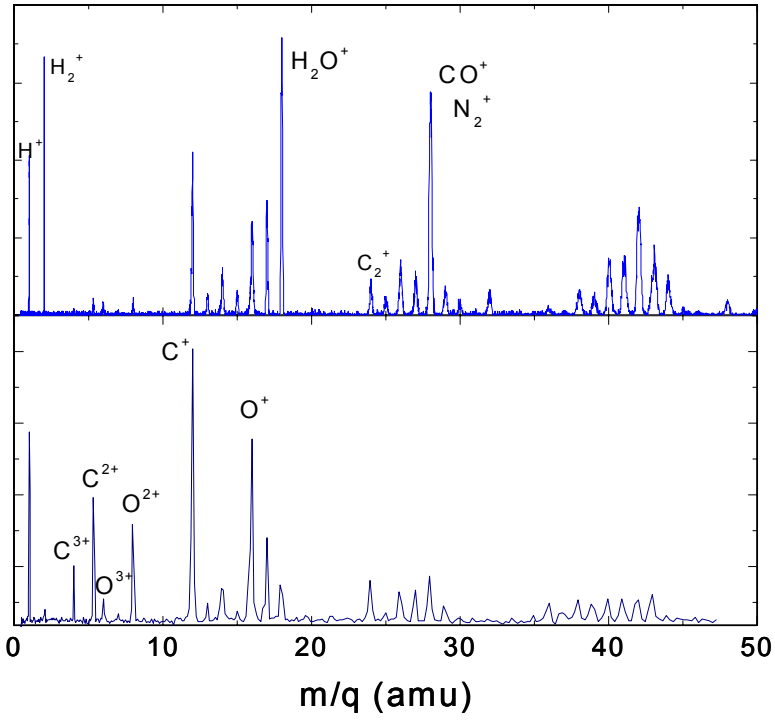

Figure 3 Chopper-ion (top) and electron-ion (bottom) coincidence spectra for 12 kV O^{6+} collisions with uracil.

References

[1] O. Hadjar, R. Hoekstra, R. Morgenstern, T. Schlathölter, *Phys. Rev. A* **63** (2001) 033201
[2] T. Schlathölter, R. Hoekstra and R. Morgenstern, *J. Phys. B: At. Mol. Opt. Phys.* **31** (1998) 1321
[3] T. Schlathölter, O. Hadjar, R. Hoekstra and R. Morgenstern, *Phys. Rev. Lett.* **82** (1999) 73
[4] O. Hadjar, P. Földi. R. Hoekstra, R. Morgenstern and T. Schlathölter, *Phys. Rev. Lett.* **84** (2000) 4076

Email: tschlat@kvi.nl
Homepage: http://kvip56.kvi.nl